Verteporfin attenuates cardiac fibrosis after myocardial infarction by suppressing the YAP-Smad2/3 signaling pathway

Pei Zhang (280235766@qq.com)
The Affiliated Hospital of Southwest Medical University https://orcid.org/0000-0003-3345-8352
Ruili Liao
The Affiliated Hospital of Southwest Medical University
Yang Gan
The Affiliated Hospital of Southwest Medical University
Hui Liu
The Affiliated Hospital of Southwest Medical University
Liang Mao
The Affiliated Hospital of Southwest Medical University
Yongmei Nie
The Affiliated Hospital of Southwest Medical University
Fengxu yu
The Affiliated Hospital of Southwest Medical University
Mingbing Deng
The Affiliated Hospital of Southwest Medical University
Bing LIAO
The Affiliated Hospital of Southwest Medical University
Yong Fu
The Affiliated Hospital of Southwest Medical University

Research Article

Keywords: Verteporfin, Myocardial infarction, Cardiac fibrosis, YAP-Smad2/3 signaling pathway

Posted Date: March 16th, 2023

DOI: https://doi.org/10.21203/rs.3.rs-2664131/v1

Abstract

Purpose

Excessive cardiac fibrosis and remodeling occur after myocardial infarction. Yes-associated protein (YAP) is a major transcriptional co-activator of the Hippo pathway and an important regulator of cardiac fibrosis. Verteporfin is a pharmacological inhibitor of YAP that effectively inhibits fibrosis and inflammatory responses. Therefore, this study aimed to explore the effects of verteporfin on cardiac fibrosis after myocardial infarction (MI) and its possible mechanisms.

Methods

Wild-type C57BL/6J mice were subjected to MI by ligating their left anterior descending coronary artery (LAD) and treating them with verteporfin (50 mg/kg/48 h) or phosphate-buffered saline for 2 weeks. Echocardiography was performed to evaluate cardiac function after 2 weeks, and hematoxylin and eosin and Masson staining were performed to evaluate the degree of myocardial fibrosis and inflammatory response. The protein expression levels of the YAP-Smad2/3 pathway, inflammatory factors, and fibrosis markers in the heart and *in vitro* were determined using western blotting and immunofluorescence staining.

Results

Compared to the MI group, verteporfin treatment improved cardiac function and fibrosis in mice post-MI. Moreover, myocardial YAP and SMAD2/3 expression were reduced in verteporfin-treated animals. Hematoxylin and eosin staining and molecular examination showed inflammatory factor and cardiac fibrosis marker expression in the heart sections.

Conclusion

Verteporfin can attenuate cardiac fibrosis and inflammatory responses and improve cardiac function by suppressing the YAP-Smad2/3 signaling pathway post-MI.

1. Introduction

Acute myocardial infarction is the most serious type of coronary heart disease and the primary cause of mortality among affected patients [1]. A massive myocardial infarction is accompanied by cardiac remodeling and inflammatory response, which can lead to heart failure in severe cases [2]. Myocardial fibroblast proliferation induces scar tissue formation, a protective mechanism against ventricular ruptures. Excessive accumulation of collagen fibers while maintaining the integrity of the heart eventually leads to ventricular wall stiffness and a marked reduction in left ventricular diastolic and systolic

functions [3]. The rapid death of cardiomyocytes, strong inflammatory response, and substantial activation of myocardial fibroblasts are the most critical factors affecting the prognosis of myocardial infarction [4, 5].

Yes-associated protein (YAP)/TAZ is an important downstream transcription factor of the Hippo signaling pathway and participates in various biological processes such as cell death, oxidative stress, inflammation, and fibrosis [6]. Following myocardial infarction, inflammatory cells, cardiac fibroblasts, and vascular endothelial cells play an important role in regulating cardiac function through the Hippo signaling pathway [7–9]. Defective Hippo signaling has been shown to prevent cardiac fibroblast differentiation during heart development through YAP [10]. YAP protein levels were found to be significantly elevated in left ventricle tissues of heart failure cohorts when compared with those of corresponding controls [10]. In a mouse model of myocardial infarction, YAP knockdown was shown to reduce cardiac fibrosis and function by modulating fibroblast proliferation, myofibroblast transdifferentiation, and the fibroinflammatory program [11–13]. YAP has been shown to bind to the Ccl2 promoter in cardiac fibroblasts, whereas YAP overexpression promotes the expression of inflammation-related genes. Therefore, the pharmacological inhibition of Hippo signaling is considered an effective strategy for promoting recovery from heart failure [14]. Moreover, the pharmacological inhibition of Hippo signaling could be an effective strategy to combat heart failure.

Verteporfin is a pharmacological inhibitor of YAP in the Hippo pathway that disrupts the YAP-TEAD interaction. *In vivo*, verteporfin treatment modulated the Hippo pathway to inhibit fibrosis in various organs [15]. However, the effect of verteporfin on cardiac remodeling and fibrosis remains unclear. Therefore, in the present study, we employed *in vivo* and *in vitro* models to determine the effects of verteporfin on cardiac fibrosis after myocardial infarction.

2. Materials And Methods

2.1 Animal experimental protocol

Animal experiments were performed in accordance with the Act and approved by the Ethics Committee of Southwestern Medical University. All procedures were carried out according to the guide for the Care and US National Institute of Health (NIH Publication No. 85–23, revised 1996). This study has no implications for replacements, improvements, or reductions.

We used 8-week-old wild-type male C57BL/6 mice (purchased at The Animal Experimental Center of Southwest Medical University, Luzhou, China) with an average weight of 25.5 ± 1.8 g at the beginning of the experiments. The mice were maintained under a 12-h light/dark cycle, controlled temperature (19–22℃), and 40–65% humidity for 1 week before initiating the experiment.

The mice were subjected to left anterior descending coronary artery ligation to induce myocardial infarction or were sham-operated, as previously described[16], assigned to either the myocardial infarction or sham group, respectively. The myocardial infarction group received intraperitoneal (i.p.)

injections of either 50 mg/kg verteporfin (HY-B0146; MedChemExpress, USA) or PBS for 48 h. Fourteen days after administration, the hearts and blood of mice were collected for further analysis after the echocardiographic assessment of cardiac function.

All experiments were approved by the Animal Ethics Committee of the Affiliated Hospital of Southwest Medical University and conducted in compliance with the ARRIVE guidelines. The mice were handled in accordance with the National Institutes of Health guidelines for the care and use of laboratory animals.

2.2 Echocardiographic assessment

To evaluate cardiac function, all mice underwent echocardiography before surgery and two weeks after surgery. Transthoracic echocardiography was performed on conscious mice using a VisualSonics Vevo 3100 ultrasound biomicroscopy system (FUJIFILM VisualSonics, Inc., Toronto, Canada) equipped with a 40 MHz RMV 704 scan head. The percentage of fractional shortening (FS, %), ejection fraction (EF, %), left ventricular end-diastolic volume, and left ventricular end-systolic volume were measured. All measurements were performed by a trained technician and averaged for at least three consecutive cardiac cycles.

2.3 *In vitro* cell experiments

Primary cardiac fibroblasts were isolated from neonatal mouse myocardia via differential adherent culture, as described previously[17]. Briefly, hearts from neonatal C57BL/6 mice were thoroughly minced and placed in a solution containing 0.25% trypsin and 0.1% collagenase Type II (C6885, Sigma-Aldrich, USA). After centrifugation, cells were resuspended in Dulbecco's Modified Eagle Medium (DMEM) supplemented with 10% fetal bovine serum (FBS), 100 U/mL penicillin, and 100 μg/mL streptomycin. Cardiac fibroblasts were isolated and cultured at 37°C with 5% CO_2.

2.4 Cell Counting Kit (CCK) assay to determine cell viability

The CCK assay was used to determine the cytotoxic effect of verteporfin on cardiac fibroblasts. Here, cardiac fibroblasts were seeded into 96-well culture plates at a density of 5,000 cells/well and cultured with verteporfin at different concentrations for 24 h. Each group was incubated with 10 μL CCK-8 reagent at 37°C for 2 h. The absorbance was measured at 450 nm with a microplate reader, and cell viability was presented as the percentage of CCK-8 reduction relative to that of the control. Cell viability (%) was calculated using the following formula:

Cell viability (%) = (As-Ab)/(Ac-Ab) × 100%

where As represents the absorbance of the test well (including DMEM, cells, CCK, and verteporfin), Ac is the absorbance of the control well (including DMEM, cells, and CCK, but without verteporfin), and Ab is the absorbance of the blank well (including DMEM and CCK, but without cells and verteporfin).

2.5 Wound healing assay

Cells were cultured in 6-well dishes. Before treatment with verteporfin and transforming growth factor (TGF)-β1, we scratched the 6-well dishes using a sterile 200-μL pipette tip, causing three separate wounds. The cells were incubated with verteporfin (250 nM) for 30 min and then stimulated with TGF-β1 (2 ng/mL) for 24 h. Wound length was measured using ImageJ software (National Institutes of Health, Bethesda, MD). Wound length at 0 h after scratching was used as a control.

2.6 Histological analysis

Heart tissue was collected at the end of the experiment and fixed in 4% paraformaldehyde for 24 h. The next day, the tissues were processed overnight using a Leica automatic tissue processor, embedded in paraffin, and sectioned. Then, 5-μM thick histological sections were prepared using a microtome. To detect cardiac fibrosis and examine the general appearance of heart tissues, hematoxylin and eosin and Masson's trichrome staining were performed according to standard procedures.

2.7 Immunofluorescence staining

Fibroblasts were seeded on cover glasses. After fixing with 4% paraformaldehyde at 37°C for 15 min, the cells were treated with 0.1% Triton X-100 for 10 min, blocked with 5% bovine serum albumin at 37°C for 30 min, and then incubated with primary antibodies overnight at 4°C. Subsequently, fibroblasts were incubated with the corresponding fluorescently labeled secondary antibodies (FITC-conjugated goat anti-rabbit IgG) for 1 h in the dark at room temperature. Next, the cells were incubated with DAPI (G1012, Servicebio, Wuhan, China) for 10 min in the dark at 37°C. Finally, the samples were observed using a confocal laser scanning microscope.

2.8 Protein isolation and analysis

Cells and tissues were lysed using a radioimmunoprecipitation assay buffer supplemented with a protease inhibitor cocktail. Protein concentrations were determined using a bicinchoninic acid assay (BCA). Equal amounts of protein (30 μg) were subjected to sodium dodecyl sulfate-polyacrylamide gel electrophoresis (SDS-PAGE) and then transferred onto a PVDF membrane. The membranes were blocked in 5% milk/TBST for 1 h at 37°C. Subsequently, the membranes were incubated with diluted primary antibodies overnight at 4°C. The primary antibodies used were anti-collagen type I (Abcam, 1:1000), α-SMA (Abcam, 1:1000), YAP (Cell Signaling Technology, 1:1000), p-YAP(Cell Signaling Technology, 1:1000), SMAD2 (Cell Signaling Technology, 1:1000), SMAD3 (Cell Signaling Technology, 1:1000), p-SMAD2 (Cell Signaling Technology, 1:1000), p-SMAD3 (Cell Signaling Technology, 1:1000), interleukin (IL)-6 (Cell Signaling Technology, 1:1000), tumor necrosis factor (TNF)-α (Cell Signaling Technology, 1:1000), and GAPDH (Beyotime Biotechnology, 1:5000). Membranes were then incubated with the corresponding diluted horseradish peroxidase (HRP)-conjugated secondary antibodies for 1 h at 37°C, and protein blots were developed using an enhanced chemiluminescence method. The membranes were washed with 1× TBST and stripped with stripping buffer for 10 min. Next, the membranes were blocked in 5% milk/TBST for 1 h at 37°C, and the same protocol was repeated with YAP- and HRP-conjugated secondary antibodies. Bands were detected using ECL and X-ray film, quantified using densitometry relative to GAPDH expression, and relative expression was assessed.

2.9 Statistical analyses

The results are expressed as the mean ± standard error of the mean, and statistical analyses were conducted using GraphPad Prism 8.0 (GraphPad Software, Inc., La Jolla, CA, USA). The normality of the data distribution was tested using the Kolmogorov-Smirnov test. One-way ANOVA with a post-hoc Holm-Sidak test ($P < 0.05$, with no significant variance in homogeneity) was used for multiple-group comparisons.

3. Results

3.1 Verteporfin helps preserve cardiac function after myocardial infarction

To investigate the effect of verteporfin on cardiac function post-myocardial infarction, we performed animal experiments (Fig. 1A). Specifically, we performed echocardiography in mice 14 days after inducing myocardial infarction. The results showed a significant preservation of cardiac function in vehicle-treated mice when compared with that in the sham-operated group (Fig. 1B-1D), as well as a reduction in cardiac hypertrophy (Fig. 1E-1F).

3.2 Verteporfin reduces myocardial fibrosis and the expression of pro-inflammatory cytokines *in vivo.*

After myocardial infarction, massive cardiomyocyte death leads to thinning of the ventricular wall, and the resulting activation of cardiac fibroblasts leads to an excessive accumulation of extracellular matrix proteins, which in turn leads to a reduced systolic function of the heart and, eventually, heart failure. Therefore, we assessed the degree of cardiac fibrosis using α-smooth muscle actin (α-SMA), collagen type I (COL-I), and Masson staining. Based on Masson trichrome staining, the verteporfin-treated group exhibited a reduction in the collagen fiber volume fraction when compared with the myocardial infarction group (Fig. 2A-2B). Meanwhile, western blotting showed that the verteporfin-treated group had reduced α-SMA and COL-I expression compared with that in the myocardial infarction group (Fig. 2C-2D). To assess the inflammatory response in the heart after myocardial infarction, hematoxylin and eosin staining revealed obvious inflammatory cell infiltration in the myocardial infarction and treatment groups. However, treatment with verteporfin markedly reduced inflammatory cell infiltration in the infarction area (Fig. 2E). Similarly, we examined the expression of inflammation-related proteins using western blotting, which showed that verteporfin treatment significantly decreased the expression levels of IL-6 and TNF-α (Fig. 2F-2G).

3.3 Verteporfin reduces myocardial fibrosis by suppressing the YAP-Smad2/3 signaling pathway *in vivo.*

To investigate the protective effect of verteporfin on cardiac fibrosis after myocardial infarction, we evaluated the protein expression levels of key effectors of the Hippo signaling pathway. Compared with the myocardial infarction + PBS group, mice hearts of the myocardial infarction + PBS group exhibited increased fluorescence intensity of YAP and SMAD2/3 in the myocardial infarction area. Verteporfin treatment significantly decreased the fluorescence intensity of YAP and SMAD2/3 (Fig. 3A-3B). Furthermore, we used western blot analysis to evaluate the expression of p-YAP, YAP, and SMAD2/3 in heart tissue treated with PBS or verteporfin. Expression levels of p-YAP, YAP, and SMAD2/3 were increased post-myocardial infarction when compared with those in sham-operated hearts, and verteporfin treatment significantly decreased the myocardial infarction-induced increase in the expression of p-YAP, YAP, and SMAD2/3 (Fig. 3C-3F). These findings indicate that verteporfin treatment could reduce the myocardial infarction-induced expression of the YAP-Smad2/3 signaling pathway.

3.4 Verteporfin inhibits TGF-β1-induced fibrosis in cardiac fibroblasts

We also evaluated the effects of verteporfin treatment on TGF-β1-induced fibroblast migration and fibrosis in cardiac fibroblasts. First, we determined the effect of verteporfin treatment at a concentration of 1 μM on cardiac fibroblasts, which did not significantly impact viability (Fig. 4A); these results indicated that treatment with 1 μM verteporfin had no significant toxic effects on cardiac fibroblasts. In the wound healing assay, the scratch length of cardiac fibroblasts after 24 h of TGF-β1 treatment was significantly reduced when compared with that of vehicle-treated cardiac fibroblasts; verteporfin treatment decreased the TGF-β1-induced increase in cell migration (Fig. 4B-C). As shown by the immunofluorescence assay results, TGF-β1 treatment for 24 h significantly increased the number of α-SMA- and COL-I-positive cells, whereas treatment with verteporfin decreased the number of α-SMA- and COL-I-positive cells (Fig. 4D-4E). We further evaluated protein expression levels of α-SMA and COL-I and found that verteporfin treatment attenuated the expression of fibrosis-related proteins after TGF-β1 induction (Fig. 4F-4G).

We further evaluated the inflammation levels of TGF-β1-induced cardiac fibroblasts. The results showed that TGF-β1 treatment elevated levels of TNF-α, whereas verteporfin treatment attenuated the expression of this factor (Fig. 4H-4I).

3.5 Verteporfin inhibits fibrosis in cardiac fibroblasts by inhibiting the YAP-Smad2/3 signaling pathway *in vitro*

We further evaluated the effect of verteporfin treatment on the YAP/Smad2/3 signaling pathway in cardiac fibroblasts. After 24 h of TGF-β1 stimulation, the TGF-β group showed an increase in the fluorescence intensity of YAP and SMAD2/3, while verteporfin treatment significantly decreased the fluorescence intensity of YAP and SMAD2/3 (Fig. 5A-5B). We also used western blot analysis to evaluate the expression of p-YAP, YAP, and SMAD2/3 in cardiac fibroblasts. TGF-β1 increased p-YAP, YAP, Smad2, and Smad3 expression, while verteporfin treatment significantly decreased the TGF-β1-induced increase

in the expression of these proteins (Fig. 5C-5F). These data suggest that verteporfin modulates TGF-β1-induced cardiac fibroblast activation via the YAP/Smad2/3 signaling pathway.

4. Discussion

In the present study, we examined the effects of verteporfin treatment on pathological remodeling and cardiac function in a mouse model of myocardial infarction and found that treatment with verteporfin reduced infarct size after myocardial infarction, attenuated fibrosis, and protected cardiac function *in vivo* and *in vitro*.

Considering fibrosis studies examining various organs, including the lungs, liver, and kidneys, idiopathic pulmonary fibrosis, multiple models of cirrhosis, and renal fibrosis were accompanied by elevated levels of YAP [18–22]. Moreover, the extent of fibrosis was significantly reduced after pharmacological inhibition or knockdown of YAP, suggesting that the inhibiting abnormally increased YAP expression in fibrotic diseases is a promising treatment strategy.

Cardiac fibrosis is an end-stage pathological feature of several cardiac diseases. Excessive extracellular matrix deposition eventually leads to tissue stiffness, affecting cardiac systolic and diastolic function [15, 23]. After the onset of myocardial infarction, the Hippo pathway plays an important role in the process of myocardial infarction, and YAP maintains the resting state and differentiation of cardiac fibroblasts [6]. Based on the findings of the current study, YAP participates in cardiac fibrosis, and the cardiac fibroblast-specific knockdown of LATS1/2 induces marked cardiac fibrosis. In contrast, LATS1/2 knockdown inhibits YAP activity, further suppressing the transition from cardiac fibroblasts to myofibroblasts [24]. Cardiac fibroblast-specific knockdown of YAP preserved cardiac fibrosis and fibroblast functions, suggesting that cardiac fibrosis is suppressed by the endogenous Hippo-induced inhibition of YAP/TAZ [11]. This observation is consistent with our current results involving the verteporfin-induced pharmacological inhibition of YAP.

Current studies have identified multiple signaling pathways that regulate cardiac fibrosis, such as TGF-β/Smads, Notch, TLR4/MyD88/NF-κB, and the Wnt/β-catenin and MAPK pathways [25, 26]. Among these, the TGF-β1/Smads signaling pathway plays a critical role in myocardial fibrosis, and its key downstream regulator SMAD2/3 is known to crosstalk between multiple pathways [27, 28], forming YAP-SMAD2/3 complexes with YAP, thereby regulating cardiac fibrosis [29]. We observed an upregulation of YAP and SMAD2/3 expression in fibroblasts upon the TGF-β1-induced differentiation of myofibroblasts and downregulation of YAP and SMAD2/3, accompanied by attenuated fibrosis after intervention with verteporfin. Therefore, we suggest that *in vitro* inhibition of YAP activity in cardiac fibroblasts can effectively inhibit cardiac fibroblast activation.

In summary, our findings are mainly consistent with those of previous reports while affording advances in the field by demonstrating that endogenous YAP-SMAD2/3 was activated in cardiac fibroblasts during fibrosis, elucidating the pathological role of fibroblast YAP in cardiac fibrosis and dysfunction, and revealing that the pharmacological inhibition of YAP by verteporfin prevents cardiac myofibroblast

activation. Ultimately, we also provided evidence regarding a new pharmacological YAP inhibitor as a potential therapeutic agent for myocardial infarction-induced fibrosis.

Our current study demonstrated YAP-Smad2/3 activation in the Hippo pathway after myocardial infarction, suggesting that the Hippo pathway plays an important role in the development of myocardial infarction. Moreover, cardiac function and fibrosis in a mouse model of myocardial infarction could be improved by treatment with verteporfin, a pharmacological inhibitor of YAP, by inhibiting the YAP-Smad2/3 signaling pathway.

5. Conclusions

Verteporfin reduced the area of myocardial infarction, improved cardiac function, and decreased fibrosis by inhibiting the YAP-Smad2/3 signaling pathway in a mouse model of myocardial infarction. Therefore, verteporfin could be a potential therapeutic agent for fibrosis after myocardial infarction, although human assessments are yet to be undertaken.

Declarations

Funding

This work was supported by Sichuan Science and Technology Innovation Project,China (No.2022YFS0610).

Conflicts of interest

The author(s) declared no potential conflicts of interest with respect to the research, authorship, and/or publication of this article.

Availability of data and material

The data will be made available by the corresponding author upon request.

Code availability

Not applicable.

Authors' contributions

Pei Zhang: Investigation, Formal analysis, Writing – original draft. **Ruili Liao:** Writing – review & editing. **Yang Gan:** Methodology, Investigation, Data curation. **Hui Liu:** Resources, Conceptualization, Methodology. **Liang Mao:** Validation, Funding acquisition. **Yongmei Nie:** Validation, Investigation. **Fengxu Yu:** Investigation, Data curation, Formal analysis. **Mingbing Deng:** Investigation, Data curation, Formal analysis. **Bing Liao:** Writing review &editing, Project administration, Funding acquisition. **Yong Fu:** Investigation, Funding acquisition, Conceptualization, Supervision, Validation.

Ethics approval

All animal experimental protocols were approved by the Institutional Ethics Committee of Southwest Medical University(NO:20220214-005). And all procedures were carried out according to the guide for the Care and US National Institute of Health (NIH Publication No. 85–23, revised 1996).

Acknowledgments

This work was supported by Sichuan Science and Technology Innovation Project,China (No.2022YFS0610

Consent to participate

Not applicable

Consent for publication

All authors agreed to publish the article.

References

1. Joseph P, Leong D, McKee M et al. Reducing the Global Burden of Cardiovascular Disease, Part 1: The Epidemiology and Risk Factors. Circ Res. 2017;121(6):677-94. doi:10.1161/CIRCRESAHA.117.308903.
2. Prabhu SD, Frangogiannis NG. The Biological Basis for Cardiac Repair After Myocardial Infarction: From Inflammation to Fibrosis. Circ Res. 2016;119(1). doi:10.1161/CIRCRESAHA.116.303577.
3. Schäfer A, König T, Bauersachs J, Akin M. Novel Therapeutic Strategies to Reduce Reperfusion Injury After Acute Myocardial Infarction. Curr Probl Cardiol. 2022;47(12):101398. doi:10.1016/j.cpcardiol.2022.101398.
4. Frangogiannis NG. The inflammatory response in myocardial injury, repair, and remodelling. Nat Rev Cardiol. 2014;11(5):255-65. doi:10.1038/nrcardio.2014.28.
5. Ong S-B, Hernández-Reséndiz S, Crespo-Avilan GE et al. Inflammation following acute myocardial infarction: Multiple players, dynamic roles, and novel therapeutic opportunities. Pharmacol Ther. 2018;186:73-87. doi:10.1016/j.pharmthera.2018.01.001.
6. Zhang Q, Wang L, Wang S et al. Signaling pathways and targeted therapy for myocardial infarction. Signal Transduct Target Ther. 2022;7(1):78. doi:10.1038/s41392-022-00925-z.
7. Yu Y, Su X, Qin Q et al. Yes-associated protein and transcriptional coactivator with PDZ-binding motif as new targets in cardiovascular diseases. Pharmacol Res. 2020;159:105009. doi:10.1016/j.phrs.2020.105009.
8. Francisco J, Zhang Y, Jeong JI et al. Blockade of Fibroblast YAP Attenuates Cardiac Fibrosis and Dysfunction Through MRTF-A Inhibition. JACC Basic Transl Sci. 2020;5(9):931-45.

doi:10.1016/j.jacbts.2020.07.009.

9. Del Re DP. Beyond the Cardiomyocyte: Consideration of HIPPO Pathway Cell-Type Specificity. Circ Res. 2018;123(1):30-2. doi:10.1161/CIRCRESAHA.118.313383.
10. Sharifi-Sanjani M, Berman M, Goncharov D et al. Yes-Associated Protein (Yap) Is Up-Regulated in Heart Failure and Promotes Cardiac Fibroblast Proliferation. Int J Mol Sci. 2021;22(11). doi:10.3390/ijms22116164.
11. Mia MM, Cibi DM, Ghani SABA et al. Loss of Yap/Taz in cardiac fibroblasts attenuates adverse remodelling and improves cardiac function. Cardiovasc Res. 2022;118(7):1785-804. doi:10.1093/cvr/cvab205.
12. Johansen AKZ, Molkentin JD. Hippo signaling does it again: arbitrating cardiac fibroblast identity and activation. Genes Dev. 2019;33(21-22):1457-9. doi:10.1101/gad.332791.119.
13. Garoffolo G, Casaburo M, Amadeo F et al. Reduction of Cardiac Fibrosis by Interference With YAP-Dependent Transactivation. Circ Res. 2022;131(3):239-57. doi:10.1161/CIRCRESAHA.121.319373.
14. Tsai C-R, Martin JF. Hippo signaling in cardiac fibroblasts during development, tissue repair, and fibrosis. Curr Top Dev Biol. 2022;149. doi:10.1016/bs.ctdb.2022.02.010.
15. Dey A, Varelas X, Guan K-L. Targeting the Hippo pathway in cancer, fibrosis, wound healing and regenerative medicine. Nat Rev Drug Discov. 2020;19(7):480-94. doi:10.1038/s41573-020-0070-z.
16. Gao R, Shi H, Chang S et al. The selective NLRP3-inflammasome inhibitor MCC950 reduces myocardial fibrosis and improves cardiac remodeling in a mouse model of myocardial infarction. Int Immunopharmacol. 2019;74:105575. doi:10.1016/j.intimp.2019.04.022.
17. Miller CL, Cai Y, Oikawa M et al. Cyclic nucleotide phosphodiesterase 1A: a key regulator of cardiac fibroblast activation and extracellular matrix remodeling in the heart. Basic Res Cardiol. 2011;106(6):1023-39. doi:10.1007/s00395-011-0228-2.
18. Liu F, Lagares D, Choi KM et al. Mechanosignaling through YAP and TAZ drives fibroblast activation and fibrosis. Am J Physiol Lung Cell Mol Physiol. 2015;308(4):L344-L57. doi:10.1152/ajplung.00300.2014.
19. Bai H, Zhang N, Xu Y et al. Yes-associated protein regulates the hepatic response after bile duct ligation. Hepatology. 2012;56(3):1097-107. doi:10.1002/hep.25769.
20. Wang X, Zheng Z, Caviglia JM et al. Hepatocyte TAZ/WWTR1 Promotes Inflammation and Fibrosis in Nonalcoholic Steatohepatitis. Cell Metab. 2016;24(6):848-62. doi:10.1016/j.cmet.2016.09.016.
21. Zheng Z, Li C, Shao G et al. Hippo-YAP/MCP-1 mediated tubular maladaptive repair promote inflammation in renal failed recovery after ischemic AKI. Cell Death Dis. 2021;12(8):754. doi:10.1038/s41419-021-04041-8.
22. Chen J, Wang X, He Q et al. YAP Activation in Renal Proximal Tubule Cells Drives Diabetic Renal Interstitial Fibrogenesis. Diabetes. 2020;69(11):2446-57. doi:10.2337/db20-0579.
23. Brown RD, Ambler SK, Mitchell MD, Long CS. The cardiac fibroblast: therapeutic target in myocardial remodeling and failure. Annu Rev Pharmacol Toxicol. 2005;45:657-87.

24. Xiao Y, Hill MC, Li L et al. Hippo pathway deletion in adult resting cardiac fibroblasts initiates a cell state transition with spontaneous and self-sustaining fibrosis. Genes Dev. 2019;33(21-22):1491-505. doi:10.1101/gad.329763.119.
25. Li Y, Hiroi Y, Liao JK. Notch signaling as an important mediator of cardiac repair and regeneration after myocardial infarction. Trends Cardiovasc Med. 2010;20(7):228-31. doi:10.1016/j.tcm.2011.11.006.
26. Lu Y, Yang M, Peng M et al. Kuanxiong aerosol inhibits apoptosis and attenuates isoproterenol-induced myocardial injury through the mitogen-activated protein kinase pathway. J Ethnopharmacol. 2021;269:113757. doi:10.1016/j.jep.2020.113757.
27. Hu H-H, Chen D-Q, Wang Y-N et al. New insights into TGF-β/Smad signaling in tissue fibrosis. Chem Biol Interact. 2018;292:76-83. doi:10.1016/j.cbi.2018.07.008.
28. Luo K. Signaling Cross Talk between TGF-β/Smad and Other Signaling Pathways. Cold Spring Harb Perspect Biol. 2017;9(1). doi:10.1101/cshperspect.a022137.
29. Beyer TA, Weiss A, Khomchuk Y et al. Switch enhancers interpret TGF-β and Hippo signaling to control cell fate in human embryonic stem cells. Cell Rep. 2013;5(6):1611-24. doi:10.1016/j.celrep.2013.11.021.

Figures

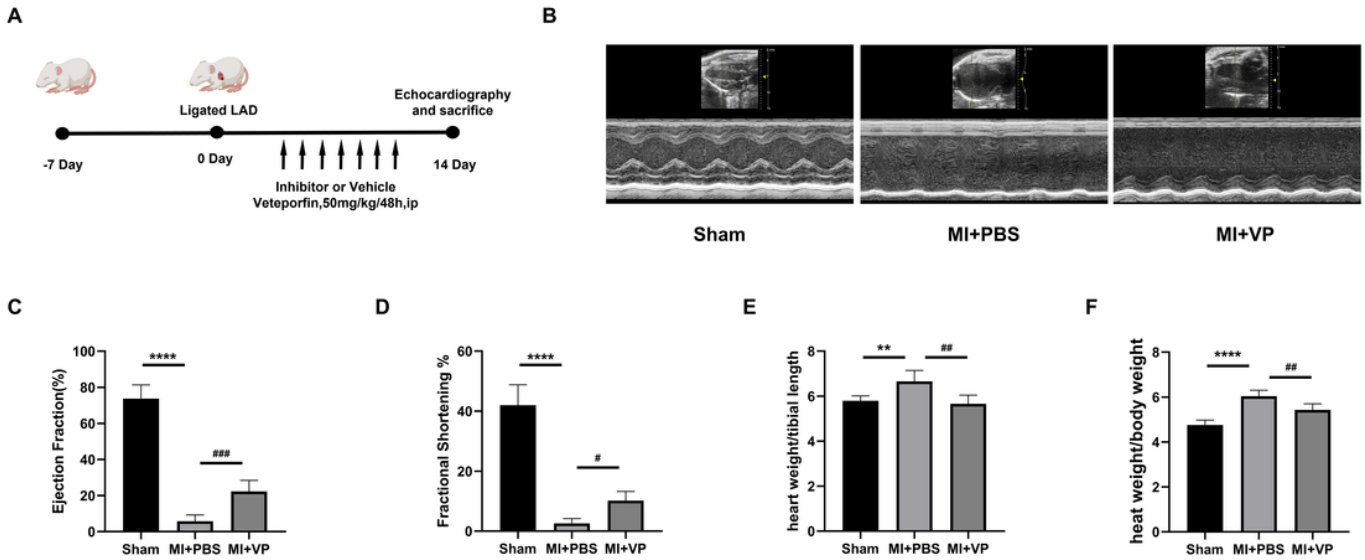

Figure 1

Verteporfin improves post-infarction cardiac function. (A) Flow chart of the intervention performed in animal experiments. **(B)** Representative M-mode echocardiographic images of each group during the

second week. **(C-D)**Summaries of the echocardiographic data of each group. **(E)** Heart weight/body weight ratio. **(F)** Ratio between heart weight and tibia length. All values are presented as the mean ± standard deviation (SD). *, P < 0.05, P < 0.01, ***, P < 0.001, ****, P < 0.0001, myocardial infarction *vs*. Sham; #, P < 0.05, ##,P< 0.01, ###, P < 0.001, ####, P < 0.0001, myocardial infarction + verteporfin *vs*. myocardial infarction + PBS. n=6.

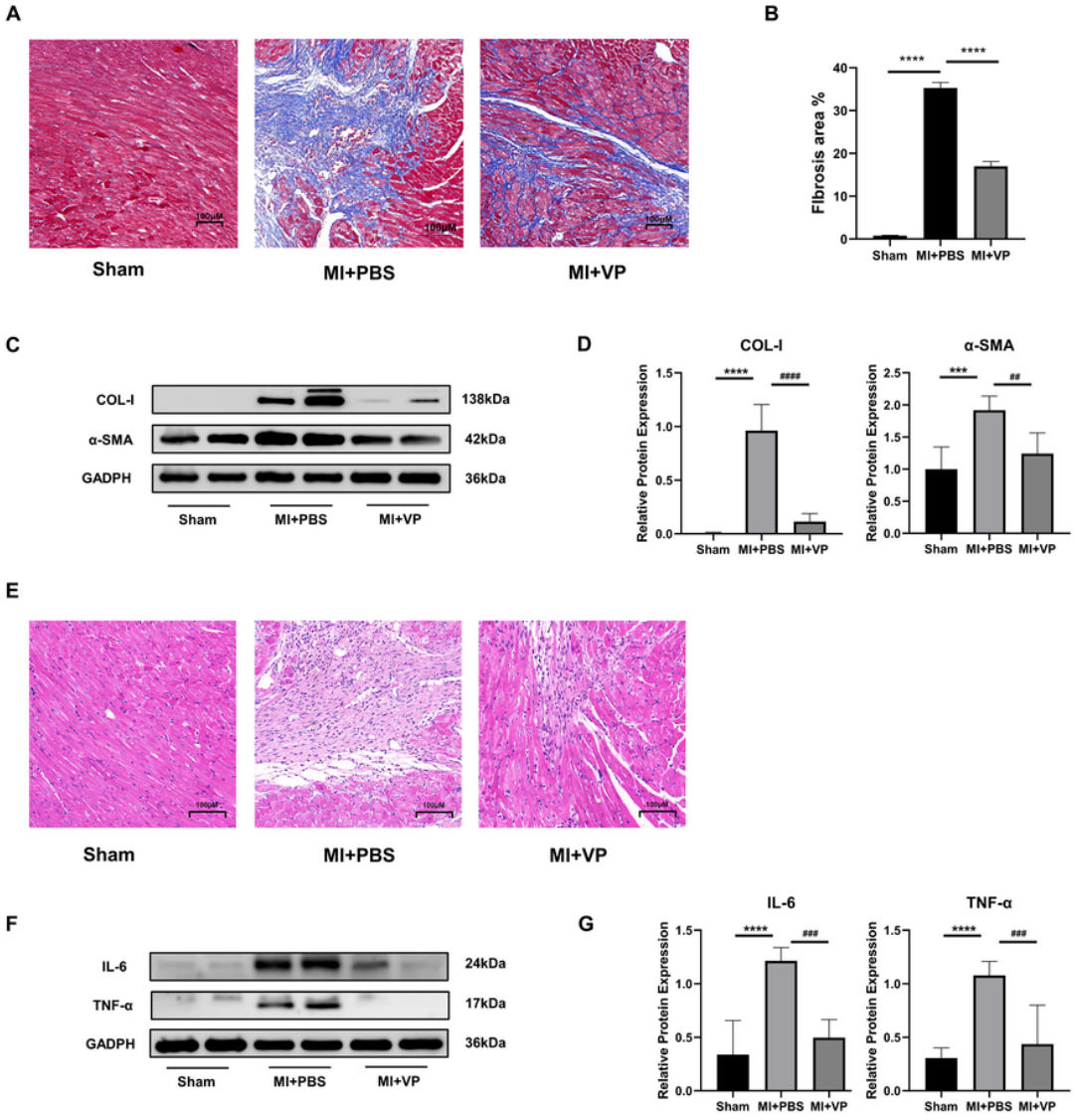

Figure 2

Verteporfin treatment attenuated cardiac fibrosis and expression of inflammatory factors *in vivo*. (A) Representative images of heart sections stained with Masson's trichrome. Blue staining shows fibrotic areas. Scale bars, 50 μm. **(B)** The percents of fibrosis area in three groups. **(C)** Representative

immunoblotting images of collagen-I, α-SMA, and GAPDH. **(D)** Gray value statistics of proteins in (C). **(E)** Representative images of heart sections stained with hematoxylin and eosin. **(F)** Representative immunoblotting images of TNF-α, IL-6, and GAPDH. **(G)** Gray value statistics of these proteins. All values are presented as the mean ± standard deviation (SD).*, P < 0.05, P < 0.01, ***, P < 0.001, ****, P < 0.0001, myocardial infarction *vs*. Sham; #, P < 0.05, ##,P< 0.01, ###, P < 0.001, ####, P < 0.0001, myocardial infarction + verteporfin *vs*. myocardial infarction + PBS. n=6. IL-6, interleukin-6; TNF-α, tumor necrosis factor-α.

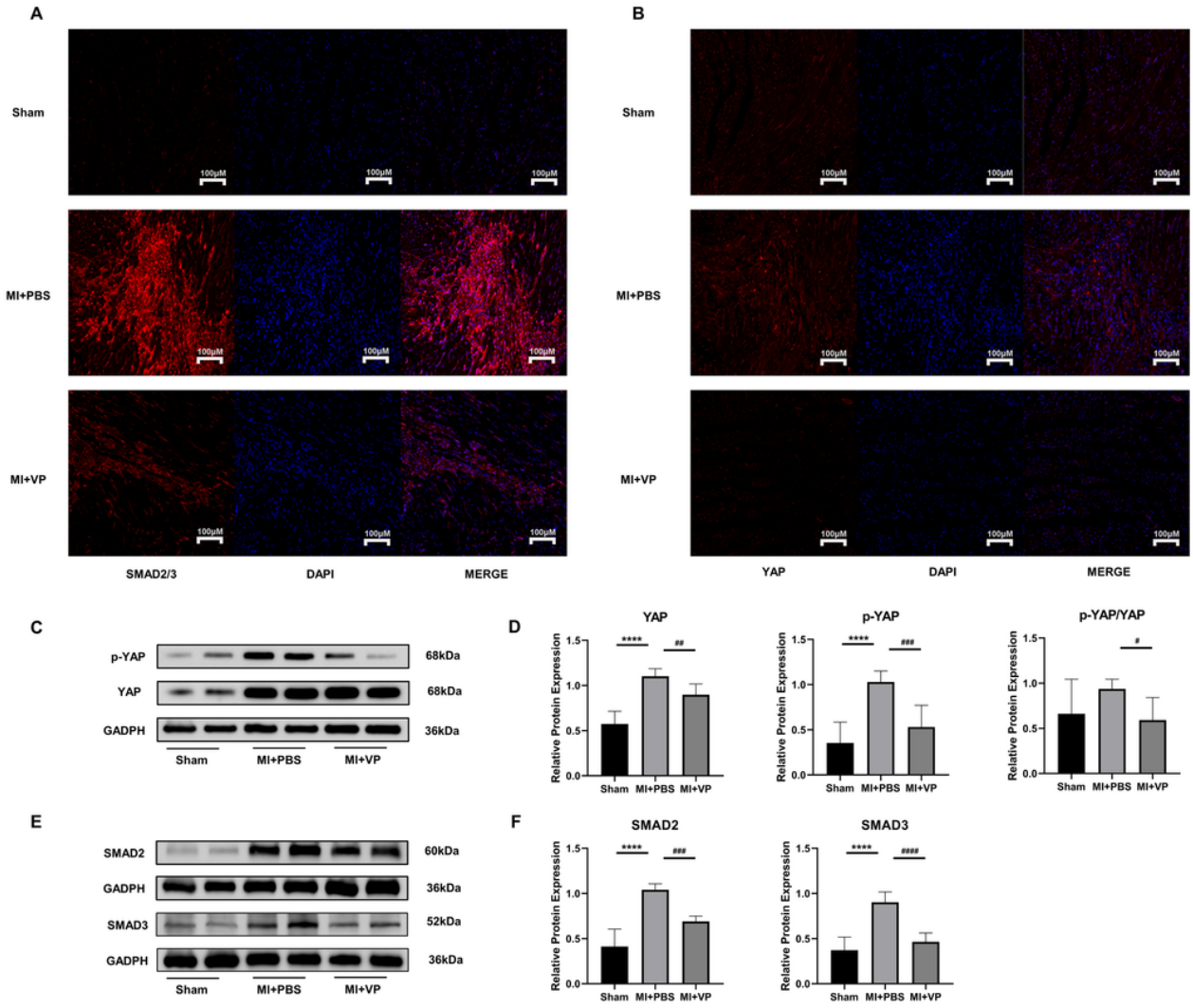

Figure 3

Verteporfin reduces myocardial fibrosis by suppressing the YAP-Smad2/3 signaling pathway *in vivo*. **(A)** Representative immunofluorescence staining images of YAP. **(B)** Representative immunofluorescence staining images of SMAD2/3. **(C)** Representative immunoblotting images of p-YAP, YAP, and GAPDH. **(D)** Gray value statistics of proteins in (C). **(E)** Representative immunoblotting images of SMAD2, SMAD3,

and GAPDH. **(F)** Gray value statistics of proteins in (E). All values are presented as the mean ± standard deviation (SD).*, P < 0.05, **, P < 0.01, ***, P < 0.001, ****, P < 0.0001, myocardial infarction *vs.* Sham; #, P < 0.05, ##, P< 0.01, ###, P < 0.001, ####, P < 0.0001, myocardial infarction + verteporfin *vs.* myocardial infarction + PBS. n=6.

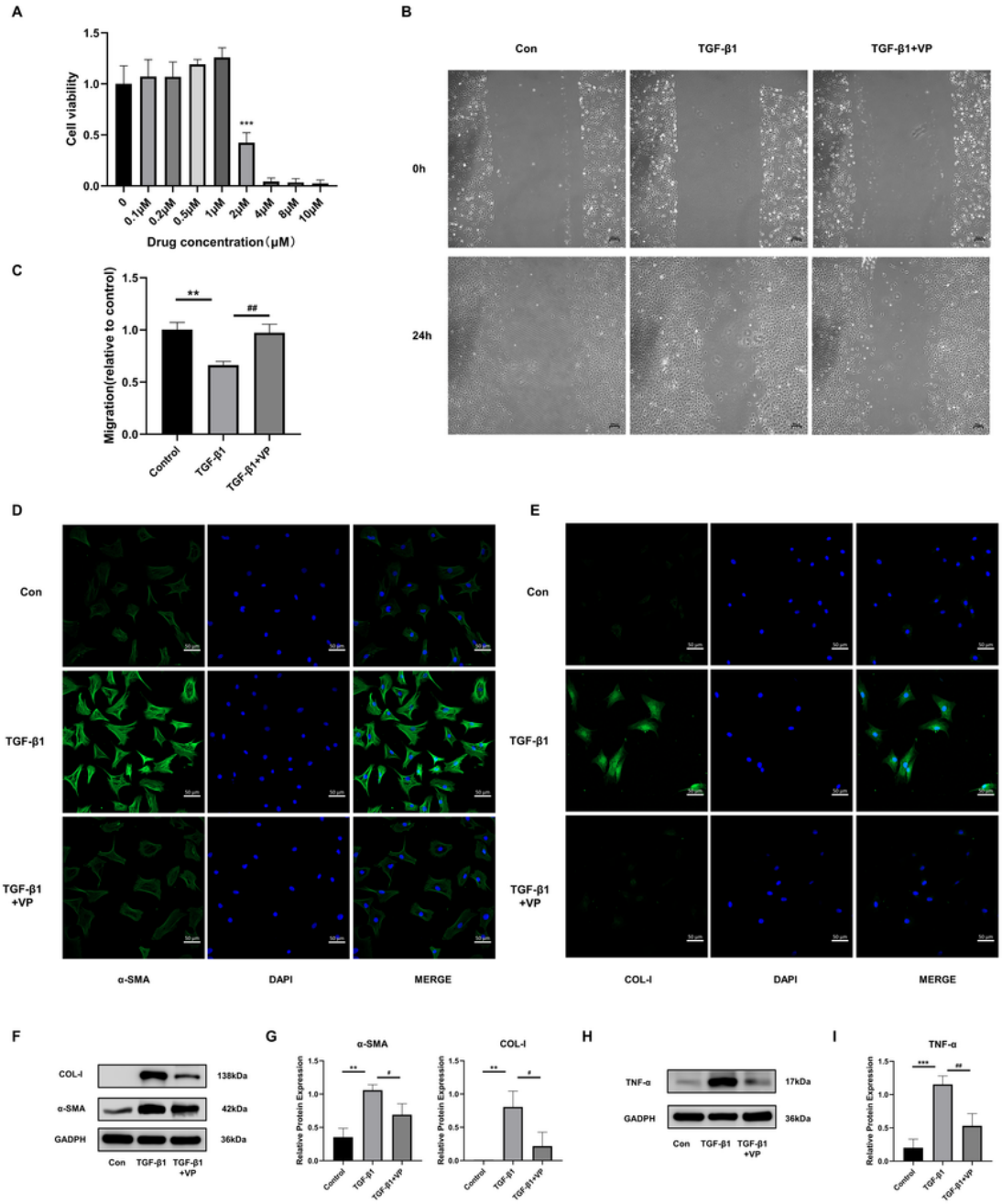

Figure 4

Verteporfin can inhibit TGF-β1-induced fibrosis in fibroblasts. (A) The effect of different concentrations of verteporfin on the viability of cardiac fibroblasts was detected using a CCK-8 assay. **(B)** Cell migration experiment. **(C)** Histograms representing the statistical analysis of the results of the migration experiment. **(D-E)** Analysis of the fluorescence intensity of COL-I and α-SMA. COL-I and α-SMA are stained green, while nuclei are stained blue. **(F)** Representative western blotting images and analysis of the protein expression of α-SMA, COL-I, and GAPDH in cardiac fibroblasts. **(G)** Gray value statistics of proteins in (F). **(H)** Representative immunoblotting images of TNF-α and GAPDH. **(I)** Gray value statistics of proteins in (H). All values are presented as mean ± standard deviation (SD). *, P < 0.05, P < 0.01, ***, P < 0.001, ****, P < 0.0001,TGF-β1 (10 ng/μL) *vs*. Control; #, P < 0.05, ##,P< 0.01, ###, P < 0.001, ####, P < 0.0001, TGF-β1 *vs*. verteporfin. n=3. α-SMA, α-smooth muscle actin; COL-1, collagen type I; TNF-α, tumor necrosis factor-α

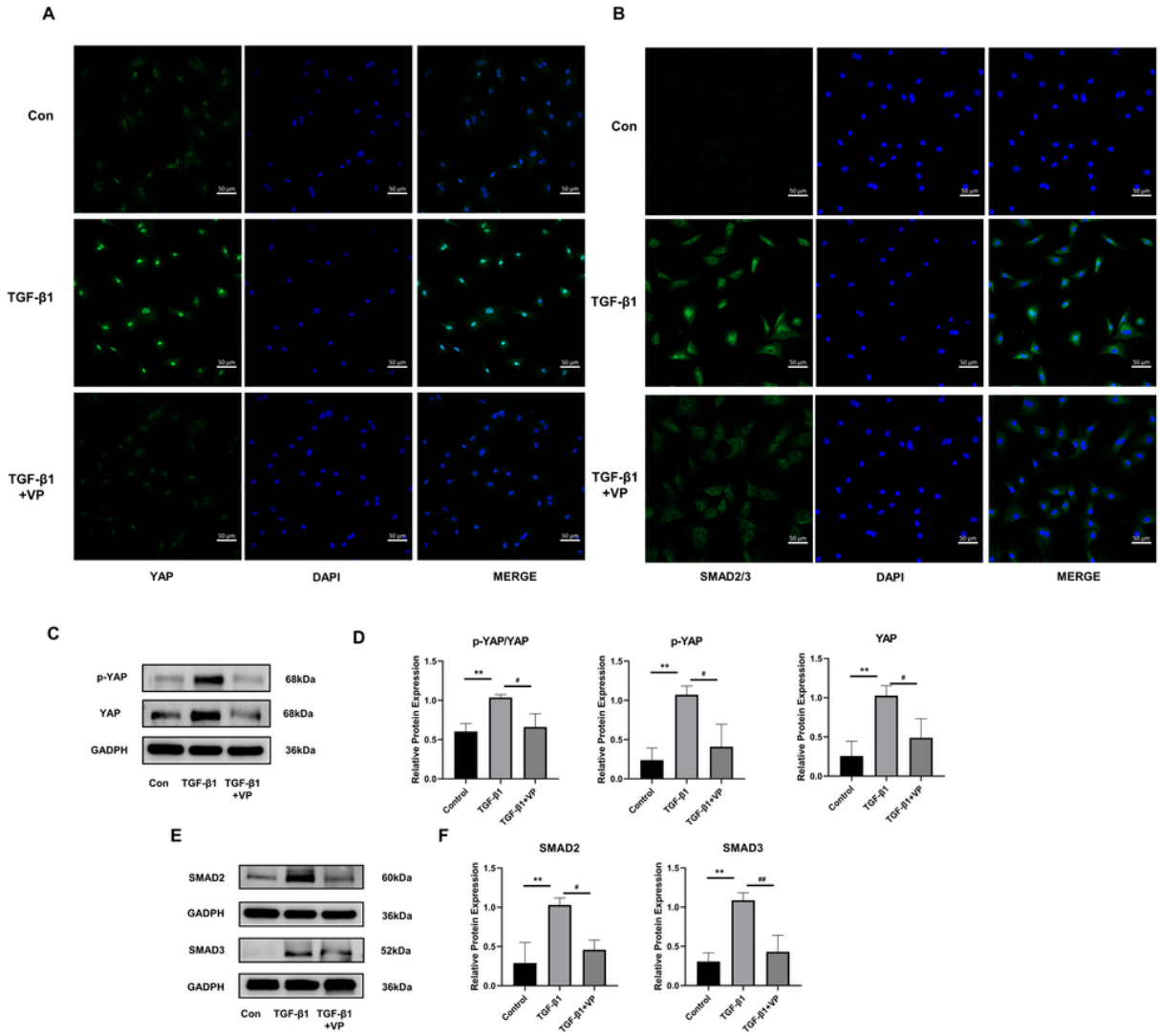

Figure 5

Verteporfin can inhibit fibrosis in cardiac fibroblasts by inhibiting the YAP-Smad2/3 signaling pathway. **(A-B)** Representative immunofluorescence staining images of YAP and SMAD2/3. **(C)** Representative western blotting images and analysis of the protein expression of p-YAP, YAP, and GAPDH in cardiac fibroblasts. **(D)** Gray value statistics of proteins in (C).**(E)** Representative western blotting images and analysis of the protein expression of SMAD2, SMAD3, and GAPDH in cardiac fibroblasts. **(F)** Gray value statistics of proteins in (E). All values are presented as the mean ± standard deviation (SD).*, P < 0.05, P < 0.01, ***, P < 0.001, ****, P < 0.0001,TGF-β1 (10 ng/μL) vs. Control; #, P < 0.05, ##,P< 0.01, ###, P < 0.001, ####, P < 0.0001, TGF-β1 vs. verteporfin. n=3.